

## The cool atmospheres of the binary brown dwarf $\varepsilon$ Indi B<sup>\*</sup>

M. F. Sterzik<sup>1</sup>, E. Pantin<sup>1,2</sup>, M. Hartung<sup>1</sup>, N. Huelamo<sup>1</sup>, H. U. Käuff<sup>3</sup>, A. Kaufer<sup>1</sup>, C. Melo<sup>1</sup>,  
D. Nürnberger<sup>1</sup>, R. Siebenmorgen<sup>3</sup>, and A. Smette<sup>1</sup>

<sup>1</sup> European Southern Observatory, Casilla 19001, Santiago 19, Chile  
e-mail: msterzik@eso.org

<sup>2</sup> DSM/DAPNIA/Service d'Astrophysique, CEA/Saclay, 91191 Gif-sur-Yvette, France

<sup>3</sup> European Southern Observatory, 85748 Garching b. München, Germany

Received 15 March 2005 / Accepted 30 April 2005

**Abstract.** We have imaged  $\varepsilon$  Indi B, the closest brown dwarf binary known, with VISIR at the VLT in three narrow-band mid-infrared bandpasses located around 8.6  $\mu\text{m}$ , 10.5  $\mu\text{m}$  and 11.3  $\mu\text{m}$ . We are able to spatially resolve both components, and determine accurate mid-infrared photometry for both components independently. In particular, our VISIR observations probe the  $\text{NH}_3$  feature in the atmospheres of the cooler and warmer brown dwarfs. For the first time, we can disentangle the contributions of the two components, and find that  $\varepsilon$  IndiBb is in good agreement with recent “cloud-free” atmosphere models having an effective temperature of  $T_{\text{eff}} = 800$  K. With an assumed age of 1 Gyr for the  $\varepsilon$  Indi system, component Ba agrees more with  $T_{\text{eff}} \approx 1100$  K rather than with  $T_{\text{eff}} = 1200$  K, as suggested by SPITZER spectroscopic observations of the combined  $\varepsilon$  Indi B system (Roellig et al. 2004). Even higher effective temperatures appear inconsistent with our absolute photometry, as they would imply an unphysical small size of the brown dwarf  $\varepsilon$  IndiBa.

**Key words.** stars: low-mass, brown dwarfs – stars: binaries: general

### 1. Introduction

$\varepsilon$  Indi B, the closest brown dwarf known (Scholz et al. 2003), has been recently discovered as a close binary, consisting of two brown dwarf components separated by 0.73'' (McCaughrean et al. 2004). The system has a well-established distance (3.626 pc, ESA 1997) and age (range 0.8–2 Gyr; Lachaume et al. 1999), and will allow the determination of fundamental physical parameters like its mass, luminosity, effective temperature, and surface gravity with unprecedented precision. Extending the analysis towards the mid-infrared (MIR) offers the opportunity to benchmark evolutionary and atmospheric models for very low temperatures.

Adaptive optics assisted near-infrared (*H*-band) low-resolution ( $R \sim 1000$ ) spectroscopy (McCaughrean et al. 2004) of both components individually lead to a most likely spectral classification of T1 for  $\varepsilon$  Indi Ba and T6 for  $\varepsilon$  Indi Bb based on the Burgasser et al. (2002)  $\text{H}_2\text{O}$  and  $\text{CH}_4$  spectral indices. Effective temperatures between 1238 K and 1312 K were derived for  $\varepsilon$  Indi Ba and between 835 K and 875 K for  $\varepsilon$  Indi Bb, bracketed by assuming the most likely ages between 0.8 and 2 Gyr. However, the comparison of high-resolution ( $R \sim 50\,000$ ) near-infrared spectra of  $\varepsilon$  Indi Ba (Smith et al. 2003) with synthetic atmosphere spectra of Tsuji (2002) leads to a much higher  $T_{\text{eff}} = 1500 \pm 100$  K. The reasons for the large

discrepancy are not known, but may be related to the radius of the brown dwarf or to uncertainties in the bolometric corrections assumed.

$\varepsilon$  Indi B has recently been observed by the SPITZER Space Telescope in the mid-infrared (Roellig et al. 2004). Their low-resolution IRS spectrum is a composite spectrum of both components, as the limited angular resolution of SPITZER does not allow to resolve it spatially. Roellig et al. claim that their observation is the first evidence for  $\text{NH}_3$  absorption in very cool brown dwarf atmospheres between 10  $\mu\text{m}$  and 11  $\mu\text{m}$ , although they cannot disentangle the contributions of both components individually. The SPITZER spectrum matches well a composite model described by Saumon et al. (2003, hereafter SML), assuming cloudless synthetic spectra.

Here, we report spatially resolved MIR photometry of  $\varepsilon$  Indi B obtained with VISIR, the new mid-infrared camera and spectrometer at the VLT (Lagage et al. 2004) during science verification. Our goal is to constrain the most pertinent brown dwarf model atmospheres with our data.

### 2. Observations

$\varepsilon$  Indi B has been imaged with VISIR mounted on the UT3 (Melipal) of the VLT on Sep. 28, 2004 (in filters PAH1 and PAH2) and on Sep. 30, 2004 (in filter SIV) under clear and stable atmospheric conditions. A nominal pixel scale of 0.075'' was used in all bands, and standard chopping and nodding

\* Based on observations collected with the ESO VLT, Paranal, Chile, program 60.A-9245(A).

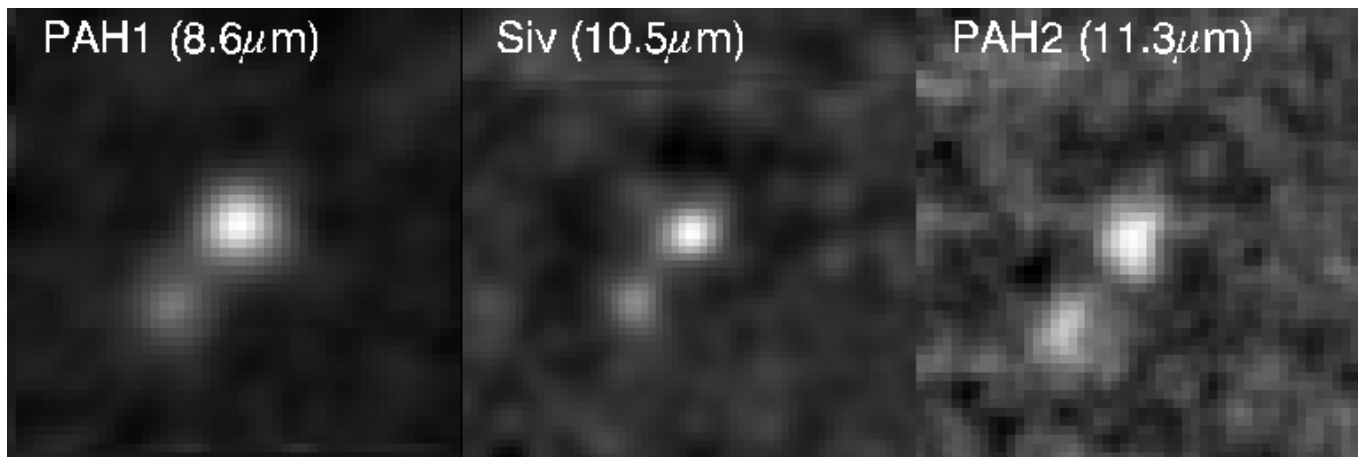


**Fig. 1.** VISIR images of  $\epsilon$  Indi B in three filters PAH1, SIV and PAH2. Components a+b are clearly resolved in all three bandpasses. North is up, and east left:  $\epsilon$  Indi Bb is the fainter source to the south-east.

**Table 1.** Log of the VISIR observations of  $\epsilon$  Indi B.

RJD	Filter	$\lambda_{\text{cen}}$	$\Delta\lambda$	AM	Int[s]	Calibrator <sup>a</sup>
53 277.6	PAH1	8.59	0.42	1.18	3638	HD 224630 HD 10550
53 277.7	PAH2	11.25	0.59	1.29	3587	HD 224630
53 279.6	SIV	10.49	0.16	1.18	3564	HD 178345

techniques ( $10''$  amplitudes) were employed. Figure 1 show the final, co-added and median cleaned images that were used for sub-sequent photometry. The binary is clearly resolved, the measured image quality ( $FWHM$ ) on the final frames is around  $0.4\text{--}0.5''$  for each point source, slightly above the diffraction limit. While the position angle from our three measurements ( $137^\circ \pm 6^\circ$ ) is consistent with that determined by McCaughrean et al. (2004) using AO one year earlier ( $136.81^\circ \pm 0.14^\circ$ ), our separation ( $0.92'' \pm 0.06''$ ) is larger ( $0.732'' \pm 0.002''$ ), and suggests orbital motion.

A summary of the observing log, filter central wavelengths, half band-width and total on-source integration times, is given in Table 1. Source count-rates were determined with standard aperture photometry. Curve-of-growth methods were applied to find the aperture radii that maximized the signal-to-noise ratio of the extracted source. Those radii were then also used for the calibration source to determine the count-rate to flux conversion factor. For faint sources, the optimal extraction aperture radius is not always well determined, and the presence of a second companion does not allow to grow the aperture to more than half of their distance. The variation of the count-rate to flux conversion factors with aperture radius was screened for aperture radii of 4, 5 and 6 pixel (corresponding to radii of  $0.3''$ ,  $0.375''$ ,  $0.45''$ ), and constitutes the main error in the *absolute flux calibration* of the targets. Different calibrator stars<sup>1</sup> observed at different airmasses give fully consistent results, and their contribution to the absolute photometric errors is negligible. *Flux ratios* between the components, and between different filter passbands can be obtained with a much higher accuracy,

<sup>1</sup> Taken from the list of Cohen et al. (1999).

**Table 2.** Mid-infrared flux densities and flux ratios of  $\epsilon$  Indi B.

Object	PAH1 [mJy]	SIV [mJy]	PAH2 [mJy]	$\frac{\text{Siv}}{\text{PAH1}}$	$\frac{\text{Siv}}{\text{PAH2}}$
Ba	$7.4 \pm .4$	$7.2 \pm .6$	$6.8 \pm .8$	$.97 \pm .02$	$1.06 \pm .03$
Bb	$3.5 \pm .4$	$3.5 \pm .8$	$5.7 \pm 1.$	$1.0 \pm .04$	$0.61 \pm .08$

as the errors are only related the spread of the count rates in the four different beams, and rather independent on the actual choice of the aperture radius. Fluxes and ratios together with error estimates are summarized in Table 2.

We note that the *combined* fluxes of components Ba and Bb agree with the spectrophotometric fluxes for the  $\epsilon$  Indi B system deduced from the SPITZER spectrum shown in Fig. 2 of Roellig et al. (2004), albeit our fluxes are on the low side of their allowed 25% error range in absolute flux calibration. Component Ba dominates the mid-infrared emission, and component Bb contributes about 1/3 to the total flux density. Our SIV filter located at a central wavelength of  $10.5 \mu\text{m}$  is particular well suited to probe the potential presence of  $\text{NH}_3$  absorption features in brown dwarf atmospheres. In fact, a significant change of the relative spectral shape between both components becomes evident in the reddest passband around  $11.3 \mu\text{m}$  (PAH2), where the flux of Bb comes close to that of Ba. The flux ratio SIV/PAH2 is small for component Bb, indicating the presence of a strong  $\text{NH}_3$  absorption band. We find no indication for strong absorption in component Ba, though.

### 3. Comparison with atmosphere models

Atmosphere models are typically calculated on a grid of  $T_{\text{eff}}/g$  pairs, for specific metallicities. Taylor (2003) lists  $[\text{Fe}/\text{H}] = 0.056 \pm 0.038$  for  $\epsilon$  Indi A; therefore we refer to solar metallicities also for  $\epsilon$  Indi B.

The object radius  $R$  is the main parameter that determines the absolute spectral flux calibration of the model atmospheres, and is obtained from evolutionary calculations. Comparing the evolutionary models of Baraffe et al. (2003) with those

**Table 3.** Brown dwarf structural parameters according to evolutionary calculations of Burrows et al. (1997) for 1 Gyr.

Object	SpT <sup>a</sup>	$T_{\text{eff}}$ [K]	$\log g$ [cm s <sup>-2</sup> ]	$\log L_{\text{bol}}$ [ $L_{\odot}$ ]	$M$ [ $M_{\text{jup}}$ ]	$R$ [ $R_{\odot}$ ]
Ba	T1	1200 <sup>b</sup>	5.1	-4.78	46	0.093
		1500 <sup>c</sup>	5.3	-4.42	59	0.090 <sup>d</sup>
		1100	5.1	-4.92	41	0.095
Bb	T6	800 <sup>b</sup>	4.8	-5.42	25	0.102

<sup>a</sup> Spectral types according to McCaughrean et al. (2003).

<sup>b</sup>  $T_{\text{eff}}$  assumed by Roellig et al. (2004).

<sup>c</sup>  $T_{\text{eff}}$  according to Smith et al. (2003).

<sup>d</sup> Smith et al. (2003) assume  $R/R_{\odot} = 0.062$  and  $L/L_{\odot} = -4.71$ .

of Burrows et al. (1997) (in the given grid of ages and temperatures), we find that their radii agree within 2%. In the following we refer to the Burrows models, only, and note that different models do not contribute significantly to uncertainties in the absolute model fluxes. In Table 3 we summarize the (sub-)stellar parameters  $\log g$ ,  $L_{\text{bol}}$  and  $R$  assuming an age of 1 Gyr for the  $\varepsilon$  Indi B system. We note, however, that the age range allowed for  $\varepsilon$  Indi implies systematic variations of the model radius. While the younger age (0.8 Gyr) increases the radius by about 3%, the older age (2 Gyr) decreases the radius by 7% for all temperatures considered here. Systematic uncertainties up to 15% are therefore implicit in the absolute normalization of the model fluxes due to the age uncertainty of  $\varepsilon$  Indi.

Burrows et al. (2003) explore the age and mass dependence of H<sub>2</sub>O, CH<sub>4</sub> and NH<sub>3</sub> molecular bands on MIR spectra of very cool brown dwarfs with  $T_{\text{eff}} \leq 800$  K. We have selected a suitable spectral model ( $T_{\text{eff}} = 800$  K,  $\log g = 5$ ) which represents a brown dwarf with a mass of  $M = 25 M_{\text{jup}}$  and an age of 1 Gyr<sup>2</sup>. For the hotter component, the cloud-free model spectrum for an age of 1 Gyr corresponding to  $M = 46 M_{\text{jup}}$  and  $M = 41 M_{\text{jup}}$  for  $T_{\text{eff}} = 1200$  K and  $T_{\text{eff}} = 1100$  K, respectively, were supplied by A. Burrows (pers. comm.). Also Allard et al. (2001) provide model atmosphere spectra in the assumed parameter range. We concentrate our comparison to their “cloudless” models, which include the effects of condensation in chemical equilibrium, but ignore the effects of dust opacities altogether. Their model spectra are freely downloadable from the web<sup>3</sup>. Finally, also SML provide MIR spectra of brown dwarfs. In fact, their cloudless synthetic spectra for  $T_{\text{eff}} = 1200$  K and  $T_{\text{eff}} = 800$  K ( $\log g = 5$ ) were combined and compared to the SPITZER spectrum in Roellig et al. (2004). Both spectra were provided to us by D. Saumon directly.

For all model spectra we calculated the expected flux densities in the corresponding VISIR filter passbands by convolving the model spectrum with the respective filter transmission profiles<sup>4</sup>. In Table 4 we summarize and compare the predicted

**Table 4.** MIR flux densities for various model atmospheres. Values printed in **boldface** are consistent with our observations within  $3\sigma$ . The 800 K models refer to  $\varepsilon$  Indi Bb, while the warmer models to Ba.

Reference	$T_{\text{eff}}$ [K]	PAH1 [mJy]	Siv [mJy]	PAH2 [mJy]	$\frac{\text{Siv}}{\text{PAH1}}$	$\frac{\text{Siv}}{\text{PAH2}}$
Allard <sup>a</sup>	800	<b>4.32</b>	<b>3.64</b>	<b>6.98</b>	0.84	<b>0.52</b>
Burrows <sup>b</sup>	800	4.76	<b>4.10</b>	<b>6.04</b>	0.86	<b>0.68</b>
Saumon <sup>c</sup>	800	<b>3.68</b>	<b>2.18</b>	<b>4.86</b>	0.59	<b>0.45</b>
Allard <sup>a</sup>	1100	8.83	8.93	12.04	<b>1.01</b>	0.74
Burrows <sup>d</sup>	1100	<b>7.96</b>	<b>8.79</b>	<b>8.83</b>	1.10	<b>1.00</b>
Allard <sup>a</sup>	1200	10.67	11.36	13.21	1.06	0.86
Burrows <sup>d</sup>	1200	9.13	10.36	9.99	1.13	<b>1.04</b>
Saumon <sup>c</sup>	1200	9.21	9.87	11.68	1.07	0.85
Allard <sup>a</sup>	1500	17.09	16.97	16.60	<b>0.99</b>	<b>1.02</b>
Allard <sup>e</sup>	1500	<b>8.11</b>	<b>8.05</b>	<b>7.88</b>	<b>0.99</b>	<b>1.02</b>

<sup>a</sup> AMES-cond models from Allard et al. (2001).

<sup>b</sup> Cloud-free model from Burrows et al. (2003).

<sup>c</sup> Cloud-free models from Saumon et al. (2003, private communication).

<sup>d</sup> Cloud-free model from Burrows (private communication).

<sup>e</sup> Assuming  $R/R_{\odot} = 0.062$ .

model flux densities for the different model atmospheres. In **boldface** we mark those values that are consistent with our VISIR measurements (Table 2) allowing for a  $3\sigma$  error range. From the comparison in Table 4 we infer that most of the available model spectra for the cooler component Bb are consistent with the *absolute* MIR photometry. They also essentially match the *flux ratios* (which are independent of absolute calibration issues like the radius assumed), but tend to underestimate the  $\frac{\text{Siv}}{\text{PAH1}}$  color. All models predict a clear signature of a more or less pronounced NH<sub>3</sub> absorption feature, which is also present in our data. The predicted absolute fluxes appear somewhat ( $\approx 20\%$ ) higher than the measured ones, but are still within the allowed error range.

The warmer component Ba is more difficult to reconcile with current models and assumptions about the  $\varepsilon$  Indi B system. While cloud-free models, assuming an age of 1 Gyr and an effective temperature of 1200 K for Ba as used by Roellig et al. (2004) agree very well with their SST/IRS spectrum, they appear only *marginally consistent with our VISIR mid-infrared photometry*. The spectral shape measured for Ba (decreasing flux with increasing wavelength) is not reflected in these models. Also, their predicted MIR fluxes are  $\approx 30\%$ – $100\%$  higher than measured in the corresponding VISIR passbands. Assuming an age of 2 Gyr – at the high limit of the allowed age range – reduces the model radius to  $R = 0.087 R_{\odot}$ , and the predicted MIR fluxes by 13%. This is not sufficient to explain the lower flux densities observed. An age of 5 Gyr with a radius of  $R = 0.082 R_{\odot}$  would be required in order to match the absolute fluxes. One straightforward way to reduce the absorption signatures of NH<sub>3</sub> is to increase the temperature of the atmosphere. In fact Allard’s et al. AMES-cond model for  $T_{\text{eff}} = 1500$  K can be considered to be fully consistent with our *relative* photometry. However, when we apply the evolutionary models of Burrows et al. (1997) with a radius of  $R = 0.09 R_{\odot}$ ,

<sup>2</sup> [zenith.as.arizona.edu/~burrows/bs1/bs1.html](http://zenith.as.arizona.edu/~burrows/bs1/bs1.html)

<sup>3</sup> [ftp.ens-lyon.fr/pub/users/CRAL/fallard/](http://ftp.ens-lyon.fr/pub/users/CRAL/fallard/)

AMES-Cond-2002

<sup>4</sup> <http://www.eso.org/instruments/visir/inst/>

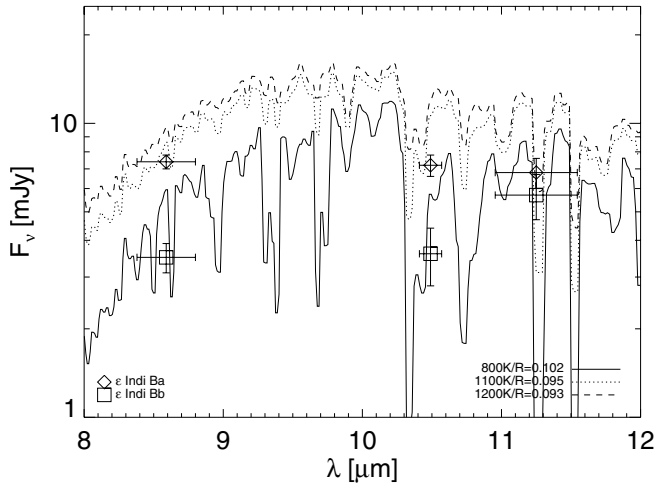


**Fig. 2.** Comparison of the VISIR photometry with various atmosphere spectra from BSL and Burrows (private communication). Radii assumed are consistent with evolutionary tracks of Burrows et al. (1997).

the *absolute* photometry is grossly off.  $T_{\text{eff}} = 1500$  K for component Ba has also been favored by Smith et al. (2003) based on the analysis of high-resolution near-infrared spectroscopy. This temperature together with the published luminosity of component Ba ( $\log L_{\text{bol}} = -4.71$ , McCaughrean et al. 2004), however, leads to a radius of only  $R = 0.062 R_{\odot}$  (Smith et al. 2003). With this smaller radius, the *absolute* VISIR photometry can now be made consistent with the spectral model. But this radius is in contradiction to all known evolutionary models (see also McCaughrean et al. 2004). Moreover, it also seems empirically unlikely in view of recent measurements of the mass-radius relation for very-low mass stars and giant planets, which prove to be similar (Pont et al. 2005). But more, direct, determinations of radii in the brown dwarf mass regime are necessary to completely rule out this possibility. As can be inferred from Table 4, both available atmosphere models with  $T_{\text{eff}} = 1100$  K tend to agree better with our measurements, assuming brown dwarf radii derived from evolutionary models at 1 Gyr. The Burrows et al. models (shown in Fig. 2 together with our photometry) for Ba seem to produce a slightly better match for the PAH2 measurement because of the presence of a strong absorption feature (that is less pronounced in the AMES-cond atmosphere).

#### 4. Summary

We report the detection of both components of  $\varepsilon$  Indi B, the closest brown dwarf binary known, with VISIR at the VLT in three narrow-band mid-infrared bandpasses located around  $8.6 \mu\text{m}$ ,  $10.5 \mu\text{m}$  and  $11.3 \mu\text{m}$ . We are able to determine accurate mid-infrared absolute photometry for both components independently, with an error level of 5–10% for the brighter component Ba, and 10–20% for the fainter Bb. Relative photometry and flux ratios can be measured with even higher accuracy. Our data show that component Bb has a prominent

absorption feature around  $10.5 \mu\text{m}$ , most likely explained by  $\text{NH}_3$ . We then compare our MIR photometry with atmospheric model spectra, using the well-known distance, metallicity and age of the  $\varepsilon$  Indi B system as main input parameters. The MIR emission of the cool component Bb appears to be fully consistent with current atmosphere models assuming an effective temperature of  $T_{\text{eff}} = 800$  K. The warmer component Ba appears only marginally consistent with  $T_{\text{eff}} = 1200$  K, a temperature that has been inferred from SPITZER spectroscopic observations of the combined  $\varepsilon$  Indi B system (Roellig et al. 2004), and from near-infrared photometry (McCaughrean et al. 2004), if we assume a canonical age of 1 Gyr for the  $\varepsilon$  Indi B system. We instead favor a slightly lower effective temperature of  $T_{\text{eff}} = 1100$  K to reconcile the absolute MIR fluxes and the spectral shape, which does not show any evidence for  $\text{NH}_3$  absorption. A higher effective temperature of  $T_{\text{eff}} = 1500$  K which would agree with the spectroscopic temperature derived for the  $\varepsilon$  Indi B system by Smith et al. (2003), implies a non-physical small radius of  $\varepsilon$  Indi Ba, and is therefore unlikely.

*Acknowledgements.* We like to thank the VISIR science verification team and the ESO director general for allocating observing time to this project. We appreciate to use the model spectra of F. Allard, A. Burrows and D. Saumon in electronic form. A. Burrows to supplied his 1100 K and 1200 K spectrum, and D. Saumon his 800 K and 1200 K model directly. The referee, A. Burgasser, helped to improve the paper.

#### References

- Allard, F., Hauschildt, P. H., Alexander, D. R., Tamanai, A., & Schweitzer, A. 2001, *ApJ*, 556, 357
- Baraffe, I., Chabrier, G., Barman, T. S., Allard, F., & Hauschildt, P. H. 2003, *A&A*, 402, 701
- Burgasser, A. J., Kirkpatrick, D. J., Brown, M. E., et al. 2002, *ApJ*, 564, 421
- Burrows, A., Marley, M., Hubbard, W. B., et al. 1997, *ApJ*, 491, 856
- Burrows, A., Sudarsky, D., & Lunine, J. I. 2003, *ApJ*, 596, 587
- Cohen, M., Walker, R. G., Carter, B., et al. 1999, *AJ*, 117, 1864
- Creech-Eakman, M. J., Orton, G. S., Serabyn, E., & Hatward, T. L. 2004, *ApJ*, 602, L129
- ESA 1997, Hipparcos and Tycho catalogues, ESA-SP 1200
- Lagage, P. O., Pel, J. W., Claret, A., et al. 2003, *SPIE*, 4841, 923
- Lauchaux, R., Dominik, C., Lanz, T., & Habing, H. J. 1999, *A&A*, 348, 897
- McCaughrean, M. J., Close, L. M., Scholz, R.-D., et al. 2004, *A&A*, 413, 1029
- Pont, F., Melo, C. H. F., Bouchy, F., et al. 2005, *A&A*, 433, L21
- Roellig, T. L., van Cleve, J. E., Sloan, G. C., et al. 2004, *ApJS*, 154, 418
- Scholz, R.-D., McCaughrean, M. J., Lodieu, N., & Kuhlbrodt, B. 2003, *A&A*, 389, L29
- Saumon, D., Marley, M. S., & Lodders, K. 2003 [[arXiv:astro-ph/0310805](http://arxiv.org/abs/astro-ph/0310805)] (SML)
- Smith, V., Tsuji, T., Hinkle, K. H., et al. 2003, *ApJ*, 599, L107
- Taylor, B. J. 2003, *A&A*, 398, 73
- Tsuji, T. 2002, *ApJ*, 575, 264